ACS OMEGA

Open Access

http://pubs.acs.org/journal/acsodf

Article

Investigating Theoretical Frameworks: Comprehending the Relationship between σ, n, and μ in MnO_2 Dispersed Films

Meenakshi, Amit Saxena, and Bhaskar Bhattacharya*

Cite This: *ACS Omega* 2023, 8, 35256−35265

Read Online

ACCESS | Metrics & More | Article Recommendations | Supporting Information

ABSTRACT: Solid polymer electrolytes (SPEs) made from a polymer−salt matrix show great potential for use in various applications, such as batteries, fuel cells, supercapacitors, solar cells, and electrochromic devices. Research on various theoretical and experimental aspects of these SPEs is highly pursued worldwide. However, due to the lack of direct experimental techniques for the measurement of the number of charge carriers (n) and their mobility (μ), reports on their correlation with conductivity (σ) and their exact theoretical justification are rare in literature studies. This paper is an attempt toward the search for the well-established theoretical formulation for n and μ that can justify the experimental results. In a previous attempt, it could only be demonstrated that the available theoretical bases show different values, but we could not come to any concrete conclusion. This research involves the use of three theoretical models, namely, the Rice and Roth model, the Trukhan model, and the Schutt and Gerdes model. The purpose of this study is to analyze the varying conductivity levels by calculating the concentration and mobility of charge carriers. To obtain the required parameters, impedance spectroscopy data were used. The Trukhan model was used to determine the precise value of the diffusion coefficient. By utilizing the dielectric tangent loss, the concentration of charge carriers and ion mobility were calculated. The Schutt and Gerdes (S&G) model was also used; this model is based on the dielectric constant and the relaxation frequency, which were derived from the EIS data. Finally, the Rice and Roth model was also employed, which is known for the ion transport in "super" ionic conductors. This was employed on the temperature-dependent impedance data for three different compositions of the films. A correlation is established between n and μ with σ using all three models. However, the Trukhan model is the most suitable for explaining the behavior of our system.

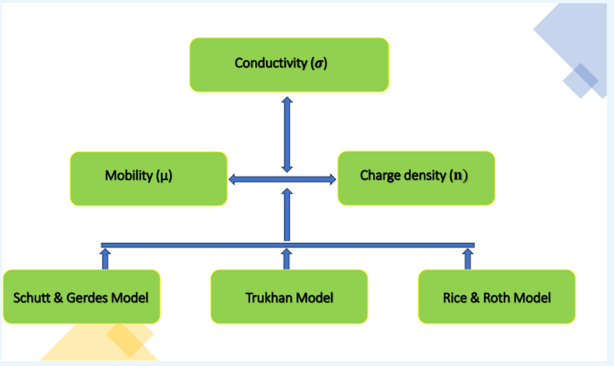

1. INTRODUCTION

Developing electrolytic materials like polymer electrolytes (PEs) is popular for the better use and enhanced performance of an electrochemical device. Due to their excellent safety, lack of leakage, broad electrochemical stability window, mechanical flexibility, and thermal stability, these polymer electrolytes are crucial components of fuel cells, supercapacitors, solar cells, and electrochromic devices. However, these polymer electrolytes require modification because their conductivity is often poor at ambient temperature. Around the world, researchers are exploring various methods to improve the conductivity of polymer electrolytes in thin films. One commonly used approach involves using inert fillers[1−3] such as Al_2O_3, SiO_2, and others.[4−6]

In the present work, we have used MnO_2 as a filler with a PEO:NaI matrix. The different weight percentages of MnO_2 are dispersed in PEO:NaI, where the cation-to-monomer ratio is kept fixed. Further, the prepared thin films were characterized for their structural and electrical studies. We have made significant calculations regarding the concentration and mobility of charge carriers in thin films, considering temperature changes. In the literature, conductivity enhancement is often emphasized as a critical factor. Nevertheless, it is equally important to consider the microscopic phenomena occurring within the composite matrix along with the increase in conductivity. The general observation of the percolation threshold was extended from crystal−crystal composites[7] to polymer−crystal composites.[8] Further variation in terms of percolation, namely, surface percolation, volume percolation, or the formation of only space charge, has been used to justify the change in conductivity. To the best of our knowledge, no attempt has been made to study the variation in the charge carrier concentration or their mobility in the polymer composite matrix.

Various articles have been published regarding the explanation of conductivity according to mobility and charge

Received: July 12, 2023
Accepted: August 22, 2023
Published: September 13, 2023

density. Rahul et al.[9] explained the variation of conductivity according to charge carriers and mobility of biopolymer electrolytes with the help of the Trukhan model. Saxena et al.[10] explained the variation of conductivity with charge density and mobility with the help of three different models: Trukhan, Schutt and Gerdes, and Rice and Roth. Hama et al.[11] explained the variation of conductivity with the Trukhan model. Gupta et al. and Munar et al. explained the variation of conductivity with the help of the Trukhan model.[12−14]

In this paper, we attempted to apply established theories of ion conduction in a glassy matrix,[15] crystalline superionic conductors,[16] and the space charge model[14] to calculate two parameters, n and μ. We extended the fundamental concepts of the abovementioned theories to a composite matrix. To understand the concept of these theoretical models, we initially calculated the conductivity (at room temperature and with temperature variation) and dielectric constant of the PE thin films, which can be seen in subsequent sections. We calculated the conductivity. The experimental data have been analyzed to establish correlations and identify any potential gaps in the models being applied. Polymer electrolytes have mobile anions and cations, with a significant portion bound by ion pairs or clusters. The total count of charge carriers can be based on the available ions, either mobile or trapped within the coil cage. This can be calculated using the Trukhan model, which uses the Nernst−Planck equations of electrodiffusion in a medium with a particular dielectric constant between two blocking electrodes.[17] The diffusion coefficients and mobile ion concentrations are then derived from the value of tan δ, where δ represents the phase angle of the complex dielectric permittivity. This indicates the availability of ions, provided that the salt is completely dissociated.

To determine the number of charge carriers using the Trukhan model, we first calculate the value of tan δ. We have calculated the charge density (D) using eq 1.

$$D = \frac{2\pi f_{\max} d^2}{32(\tan\delta)^3_{\max}} \tag{1}$$

Here, d stands for the thickness of the sample, while the values for $f_{\max}$ and $(\tan\delta)_{\max}$ are taken from the tan δ plot.

Further, the concentration of charge carriers through the Trukhan model is calculated with eq 2.

$$n = \frac{\sigma_{\mathrm{dC}} kT}{\mathrm{De}^2} \tag{2}$$

Here, σ_{dC} is the conductivity, k is the Boltzmann constant, and T is the temperature.

The Schutt and Gerdes (S&G) model is based on the concept that the matrix is amorphous and the charge carriers move under the influence of an electric field. It mainly depends on the dielectric constant and frequency of the measurement.[9] The concentration of free charge carriers (n_{SG}) is extracted from the impedance spectroscopy spectrum with the help of eq 3.

$$n_{\mathrm{SG}} = \left[\frac{\sigma}{3\epsilon_0 \epsilon'_s \omega_x}\right]^4 \frac{\epsilon'_s \epsilon_0 k_{\mathrm{B}} T}{e^2 d^2} \tag{3}$$

where σ stands for dc conductivity, ϵ_s is a real part of permittivity at high frequencies, k_{B} stands for the Boltzmann constant, ϵ_0 is the permittivity in vacuum, and "d" denotes thickness. Here, ϵ'_s is the dielectric permittivity (real part) in the high-frequency region, and ω_x stands for angular frequency, where $\epsilon\ (\omega_x) = 10\epsilon_s$, the value of the concentration of charge carriers and ion mobility.[18]

However, in general, the polymer electrolytes are not fully amorphous. The matrix is partially crystalline at room temperature. Earlier, it was observed that ions can only move in the amorphous region. However, Bruce et al. already established that ions can migrate very well in the crystalline regions,[19] but the conductivity remains low. Therefore, it becomes an over-expectation that the matrix is amorphous, and blindly applying the S&G theory may result in a value of n that is often more than Avagadro's number. This is generally attributed to a lack of understanding of the theory. However, this happens due to the assumption that the entire matrix is amorphous. To understand how the crystalline regions affect conductivity, it is important to take into account their contribution with respect to the amorphous regions. The Rice and Roth model is currently being investigated for this purpose.[20] This model is based on the idea that during a thermally active process, a transition from one site to another occurs within a fixed amount of time. This process determines the hopping frequency and the mean free path, which is the distance between one site and another.[21]

The Rice and Roth model states that the concentration of charge carriers, which can be determined using eq 4, is crucial in understanding the charge transport characteristics of polymer electrolytes.

$$\sigma = \frac{2}{3}\left[\frac{(Ze)^2}{k_{\mathrm{B}} T m}\right] n_{\mathrm{RR}} E_{\mathrm{a}} \tau \exp\left[\frac{-E_{\mathrm{a}}}{k_{\mathrm{B}} T}\right] \tag{4}$$

where Z stands for the valency of charge, m denotes the conducting ion's mass, n_{RR} stands for the mobile ion concentration, K_{B} stands for the Boltzmann constant, and E_{a} is the activation energy. However, τ is the free ion lifetime and can be obtained from the mean free path relation $\tau = \frac{l}{v}$. Here, l is the mean free path.

2. EXPERIMENTAL SECTION

For the film preparation, we utilized the standard solution casting technique, where PEO and NaI were dissolved in acetonitrile using a fixed ratio of 90:10. The solution was stirred for 10−12 h to ensure a homogeneous mixture and then poured into a polypropylene Petri dish. The solution was left to evaporate slowly at room temperature, resulting in self-supporting films. From this initial film, we obtained the reference polymer electrolyte film, which was used to analyze the changes caused by the addition of MnO_2 to subsequent thin films. To make the MnO_2-dispersed thin films, we repeated the process as mentioned above and added various wt % of MnO_2 to the PEO:NaI mixture. We prepared different MnO_2 thin films with weight percentages ranging from 0.1 to 5 wt %.

For calculating conductivity, we have used eq 5.

$$\sigma = \frac{l}{AR} \tag{5}$$

where σ is the conductivity of the polymer electrolyte, R is the bulk resistance, and A is the area of the sample.

X-ray diffraction (XRD; Empyrean and PANalytical) and FTIR (Bruker FTIR spectrophotometer, α II) analyses were carried out at room temperature to examine the structural

https://doi.org/10.1021/acsomega.3c05006
ACS Omega 2023, 8, 35256−35265

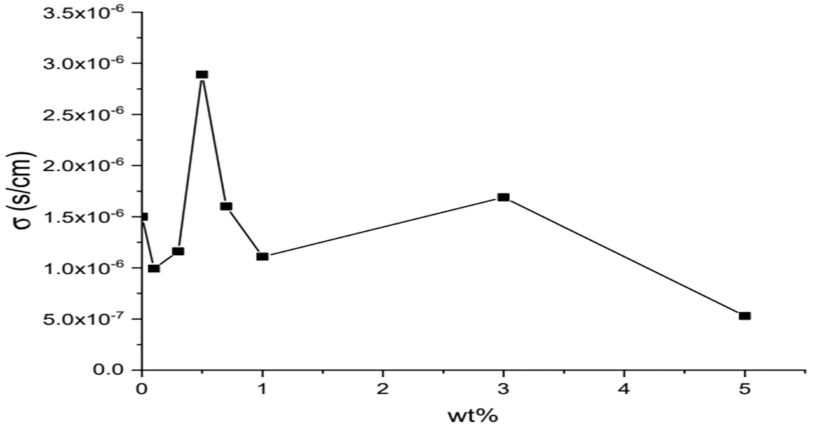

Figure 1. Conductivity variation with different wt % of MnO_2 at room temperature.

alterations in manufactured materials. Complex impedance spectroscopy (CHI 660E) was employed in the frequency range of 10^2−10^5 Hz at room temperature as well as at increasing temperatures (ranging from 30 to 110 °C), utilizing an indigenously manufactured temperature-controlled furnace to analyze the variations in the conductivity of polymer electrolyte films with temperature. The dielectric behavior, concentration, and mobility of the ions in the polymer matrix were determined using the impedance spectroscopy data. At the same time, impedance data were also used to analyze the dielectric relaxation and modulus behavior of the doped films.

3. RESULTS AND DISCUSSION

3.1. Electrical Studies. *3.1.1. Conductivity: At Room Temperature.* As shown in Figure 1, the conductivity of the polymer thin films changes at room temperature with different wt % of MnO_2. Initially, with the dispersion of MnO_2, the conductivity decreases, then gradually increases, and eventually reaches the maximum value of 2.89×10^{-6} S/cm at 0.5 wt % MnO_2. However, it starts to decline again, going through a broad peak and reaching its lowest value of 5.28×10^{-7} S/cm at 5 wt % MnO_2. It is important to note that the film was not cast beyond 5 wt % due to concerns about the uniformity of MnO_2 dispersion.

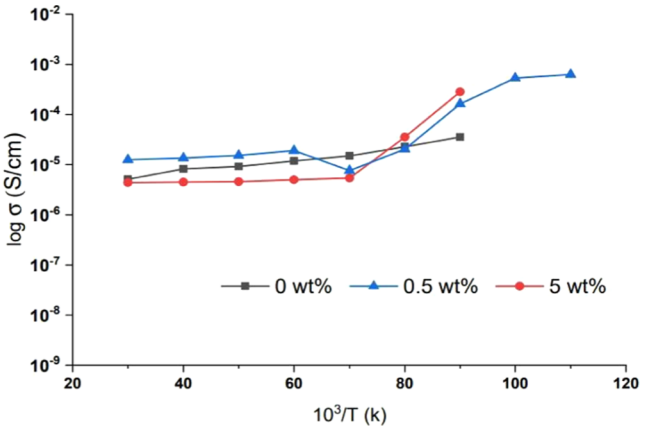

Figure 2. Temperature-dependent conductivity plot for MnO_2-dispersed PEO:NaI thin films.

The initial maxima at 0.5 wt % MnO_2 in the conductivity indicate the percolation threshold at which a charged pathway becomes available for the ions to migrate from one end to the other. This type of behavior is common in composites, and it is widely reported in the literature that conductivity improves when oxides are dispersed in PEO-based polymer electrolytes.[4,22,23] This may be due to surface or volume percolation, which is possible in this case due to the semiconducting nature of the dispersoids (MnO_2).[10,24] However, this data cannot quantify the actual reason for the increase in conductivity, whether it is the charge carrier density or their mobility. If the amount of MnO_2 is further increased, the space charge path no longer remains continuous, and conductivity decreases (at 1 wt %).

Further, with a higher wt % of MnO_2, the amorphicity of the matrix increases. This increase is independent of the charge percolation and hence should depend on the mobility of the charge carriers. In subsequent sections, the roles of n and μ have been discussed and correlated with the conductivity pattern. The second broad peak may be attributed to the percolation threshold due to the other types of charge carriers.[24] In our case, the first one is expected due to Na+, which has smaller ionic radii and is expected to move faster. The second one may be due to the iodine ions. Since iodine is known to exist in different charge states, and therefore, a broad peak is expected (can be seen in Figure 1). However, there is no experimental verification that can identify the ions responsible for the two peaks.

3.1.2. Conductivity: With Temperature Variation. The conductivities of these three samples were examined in the temperature range of 30−110 °C in order to comprehend how conductivity behaves as the temperature increases (i.e., from room temperature to above the melting point). The three chosen compositions are 0, 0.5 wt %, which shows maximum conductivity at room temperature, and 5 wt %, which is far away from the maxima. The variation of conductivity with temperature variation for 0, 0.5, and 5 wt % MnO_2 is shown in Figure 2.

As the temperature increases, the polymer chains gain quicker internal modes of vibration and facilitate polymer chain segmental motion, which in turn improves the hopping of ions through interchain and intrachain movement. As a result, ionic conductivity increases. Once the crystalline parts melt, the conductivity jumps up, as expected. These data are further used for calculating n and μ by the three models, namely, the Trukhan model, the Rice and Roth model, and the Schutt and Gerdes model.

https://doi.org/10.1021/acsomega.3c05006
ACS Omega 2023, 8, 35256−35265

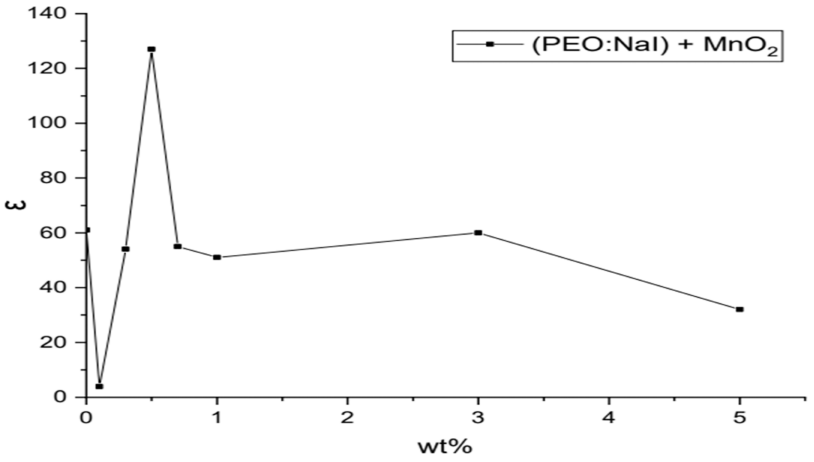

Figure 3. Variation in the dielectric constant with different wt % of MnO_2.

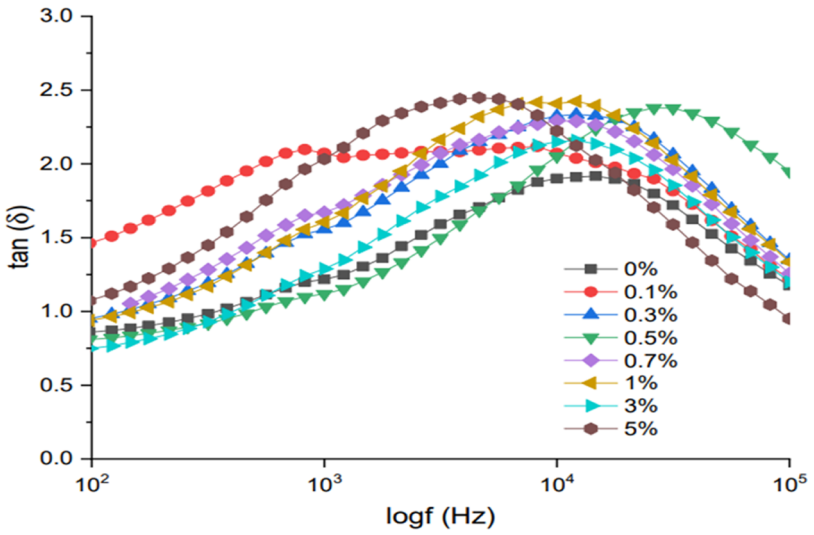

Figure 4. Graph between tan (δ) and log f for $(\tan \delta)_{max}$ and f_{max} for different wt % of MnO_2.

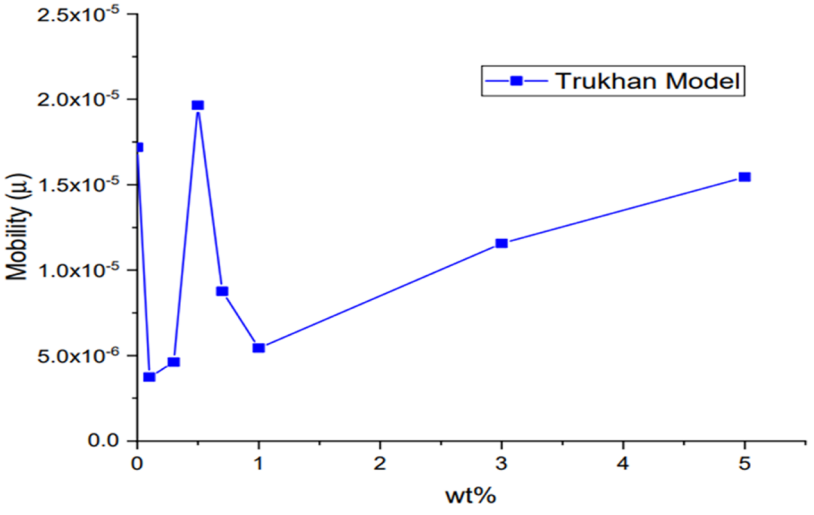

Figure 5. Mobility variation with different wt % of MnO_2 at room temperature (by the Trukhan model).

3.1.3. Dielectric Study. Using the impedance data, the films' dielectric constant was estimated. As shown in Figure 3, the dielectric constant first decreases and then attains a maximum value at 0.5 wt % MnO_2, and after that, it starts decreasing. The dielectric constant shows similar behavior to the conductivity of the films. This is obvious, as the dielectric constant directly measures the accumulation of charges in the matrix[4,25] and supports the formation of charged pathways around the MnO_2

https://doi.org/10.1021/acsomega.3c05006
ACS Omega 2023, 8, 35256−35265

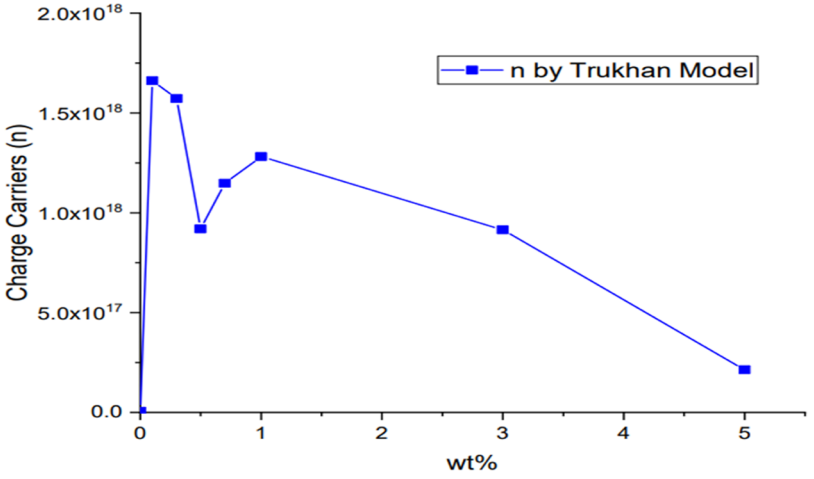

Figure 6. Concentration of charge carriers with different wt % of MnO_2 at room temperature (by the Trukhan model).

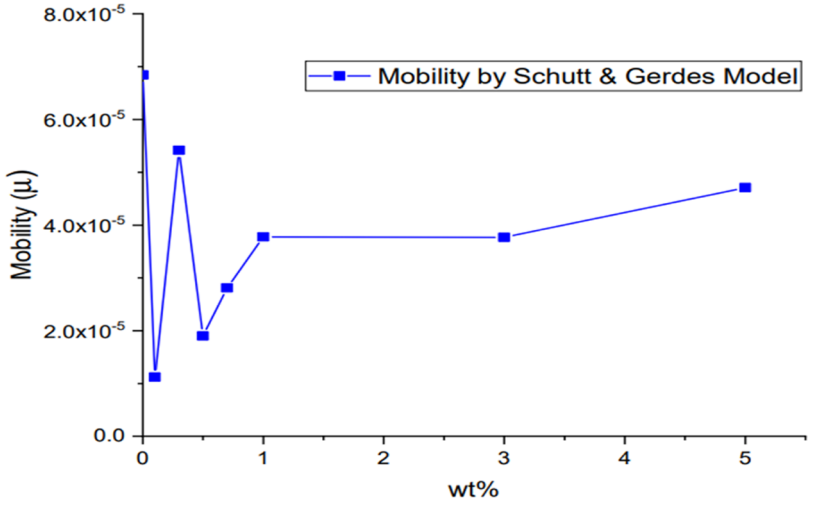

Figure 7. Mobility variation with different wt % of MnO_2 at room temperature (by the Schutt and Gerdes model).

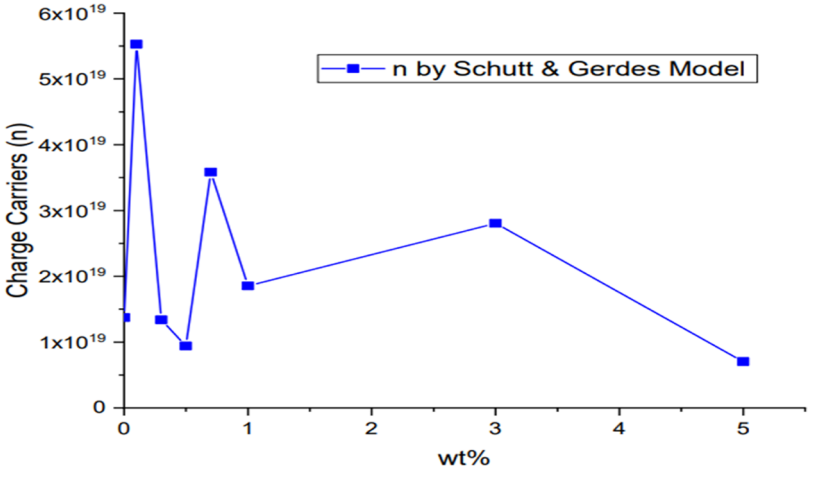

Figure 8. Concentration of charge carriers with different wt % of MnO2 at room temperature (by the Schutt and Gerdes model).

surfaces. Therefore, the possibility of surface percolation dominates but needs further confirmation. Saxena et al. and Singh et al. also showed that the dielectric constant well matched the ionic conductivity.[8,26] By adding different wt % of the MnO_2 filler, amorphicity increases and, as a result, the dielectric constant increases. Then, after 0.5 wt %, crystallinity increases as a result dielectric constant decreases.

3.1.3.1. Concentration and Mobility: At Room Temperature. The ion mobility and their concentration at different compositions at room temperature were calculated using the Trukhan model. For this, tan δ was calculated from the

https://doi.org/10.1021/acsomega.3c05006
ACS Omega 2023, 8, 35256−35265

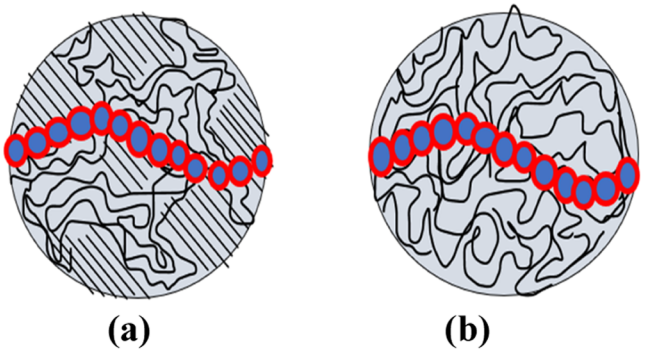

Figure 9. Representation of formation of the percolation path (a) without and (b) with MnO_2.

impedance data over the frequency range of measurement (10^2–10^5 Hz). The tan δ, n, and μ are shown in Figures 4, 5, and 6, respectively.

Upon analyzing Figures 5, 6, and 1, it is evident that the conductivity initially correlates with the mobility until it reaches 1 wt % when it starts to follow the charge concentration pattern. The carrier concentration increases and then decreases as more MnO_2 is added, possibly due to the fillers causing a change in crystallinity. The introduction of MnO_2 causes the polymer–salt complex's crystalline sections to unravel, resulting in increased amorphicity. This exposes more polymer coils and ions, enabling greater conduction and more charge carriers. However, when the dispersoid exceeds 3 wt %, the matrix's amorphicity becomes too high, resulting in the formation of an ion multiple. As a result, the matrix's conductivity decreases.[8,27,28] The variation in n can be directly explained in terms of the ion association theory.[6]

The impedance data were further used for calculating n and μ using the Schutt and Gerdes model, as shown in Figures 7 and 8. Interestingly, the charge carrier concentration at higher MnO_2 concentrations matches the conductivity pattern. The possible reason may be the concept on which this theory was formulated. The S&G theory assumes the matrix to be purely glassy, which is possible beyond 1% in our case. Therefore, for the films where the crystallinity was higher (0–1% of MnO_2), the Trukhan model was found to be satisfactory, whereas beyond 1%, when the matrix becomes highly amorphous, it does not work. In this part, the S&G theories match well with

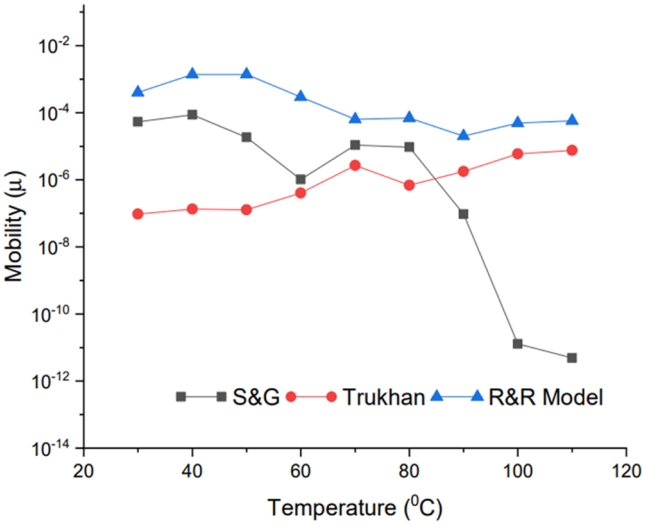

Figure 11. Variation of mobility for 0.5 wt % MnO_2 with temperature (by S&G, Trukhan, and R&R models).

the conductivity pattern. It may be noted that in S&G (Figure 7), the value of mobility becomes almost constant beyond 1%. This is possible due to the fact that once the highest state of amorphicity is obtained and all of the uncoiled chains are open, there is no further possibility of opening up the coils and hence a change in amorphicity. The initial changes in mobility can be attributed to the free movement of charges through the space charge layers created due to the interaction of the dispersoids with the matrix. The ions can freely walk through, no matter how small or large their number, through the space charge sheaths. The conductivity increases until the percolation threshold is reached. The mobility and quantity of charge carriers determine the final conductivity once the threshold has been reached.

3.1.3.2. Concentration and Mobility: With Temperature Variation. **3.1.3.2.(a) Concentration**

When we applied the Trukhan model, n was found to increase, showing a broad peak near the polymer's melting temperature. Once the polymer melts, n becomes almost constant. The concept of space charge around the MnO_2 fillers resulting in percolation pathways and thresholds can be used to understand this variation.[29] It is expected that once the

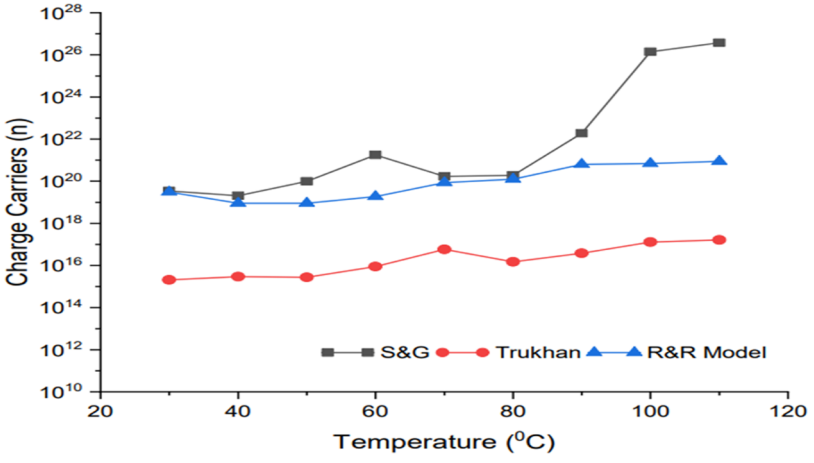

Figure 10. Variation of the concentration of charge carriers for 0.5 wt % MnO_2 with temperature (by S&G, Trukhan, and R&R models).

https://doi.org/10.1021/acsomega.3c05006
ACS Omega 2023, 8, 35256–35265

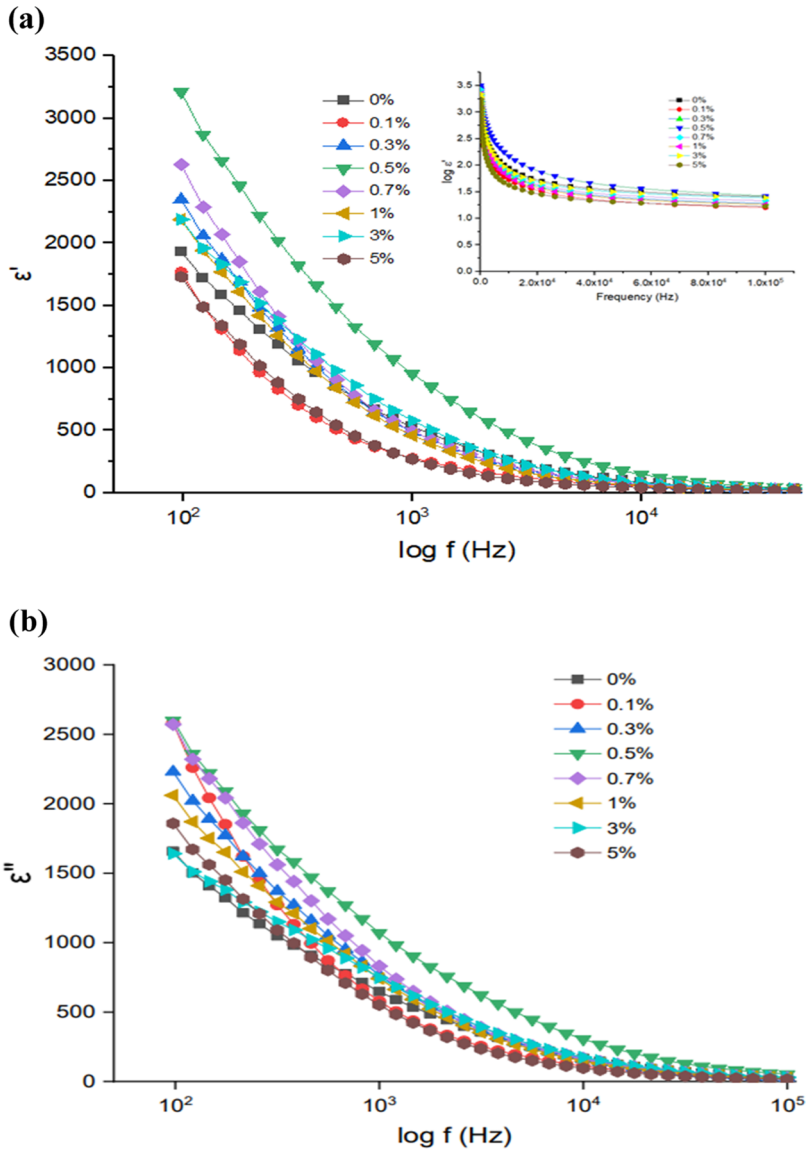

Figure 12. (a) Real part of the dielectric constant (ε') as a function of frequency for different wt % of MnO_2 (inset: log ε' vs frequency graph). (b) Imaginary part of the dielectric constant (ε'') as a function of frequency for different wt % of MnO_2.

threshold is reached, a highly conducting pathway due to space charge will be available for the mobile charge carriers. If, at melting, more charge carriers become free, they move along this pathway, and conductivity increases. However, there will be no change in the space charge regions, as shown in the schematic diagram in Figure 9. Therefore, the increase in n is less appreciable than expected.

The number of charge carriers exhibits the exact same pattern as crystallinity when we apply the S and G models. The shift in crystallinity that causes an increase in the amorphous character of the entire matrix is reflected in n because the model is based on the glassy matrix (charge carriers). The melting of the crystalline portion of the polymer−salt complex is represented by a modest peak at around 60 °C, and the melting of the crystalline PEO network is represented by a rapid rise at about 70 °C. These two melting processes, as separate, can be seen in the literature for PEO-based polymer electrolytes.[23] For further confirmation, a DTA scan (given in the Supporting Information) in this temperature region (30−110 °C) was done for this sample. A wide peak with an onset before 60° was observed. However, in the case of the sample without MnO_2, the onset was beyond 60°, which corresponds to the melting of the crystalline PEO matrix. Further comparison between the area of the two peaks also indicates that due to the addition of MnO_2, the amorphicity of the matrix increases by almost 40% with reference to the pristine sample. Therefore, in terms of the change in amorphicity of the matrix, the change in the number of charge carriers can be correlated. However, the value of n goes beyond Avagadro's number as the conductivity shouts high. Similar observations have been made for polymer electrolytes having a conductivity of approximately 10^{-3} S/cm.[30] Such a high value of n may be due to the basic consideration that the entire matrix is glassy, which is not true for polymer−salt complexes. Due to the nonavailability of any other exact model, this S&G model is still used, which can predict the values of n and μ for poorly conducting systems. However, for polymer electrolytes that may be fully amorphous, this model is limited only to the poorly conducting matrix. Otherwise, the value of n comes out

https://doi.org/10.1021/acsomega.3c05006
ACS Omega 2023, 8, 35256−35265

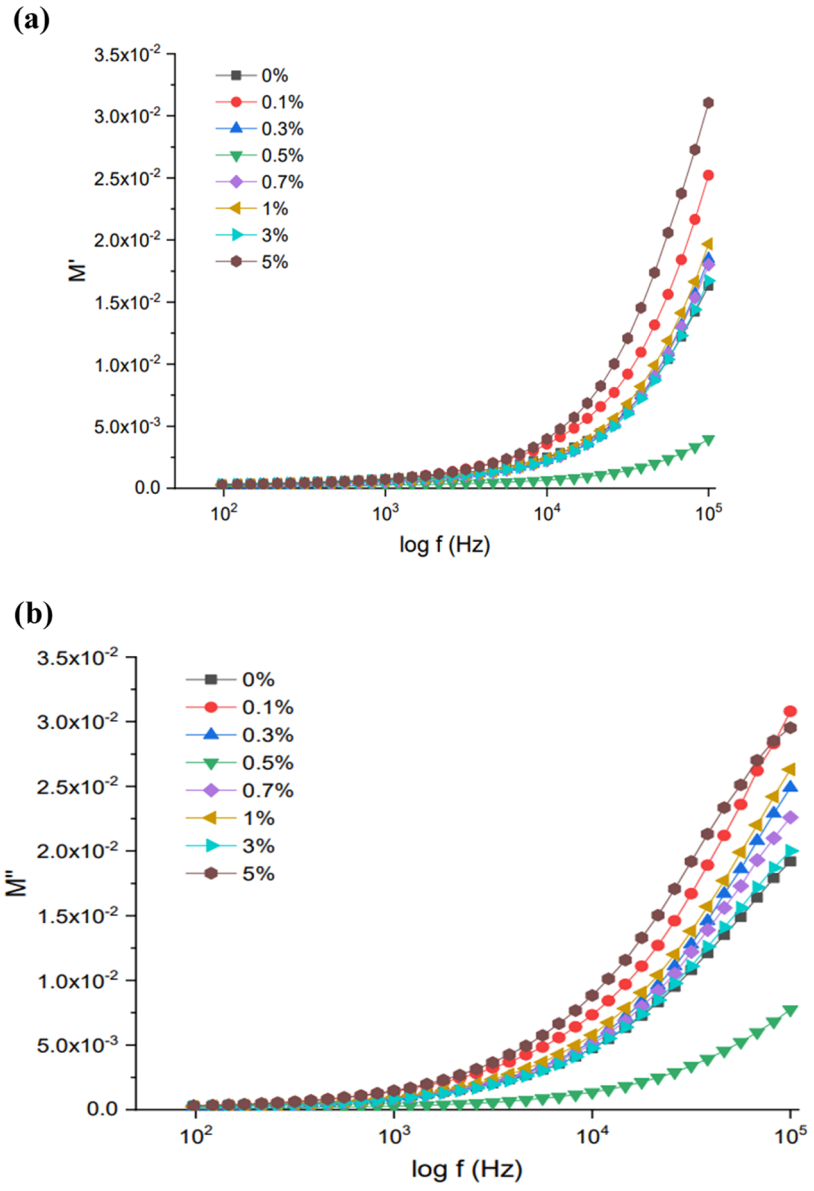

Figure 13. (a) Real part of modulus (M') as a function of frequency for different wt % of MnO_2. (b) Imaginary part of modulus (M″) as a function of frequency for different wt % of MnO_2.

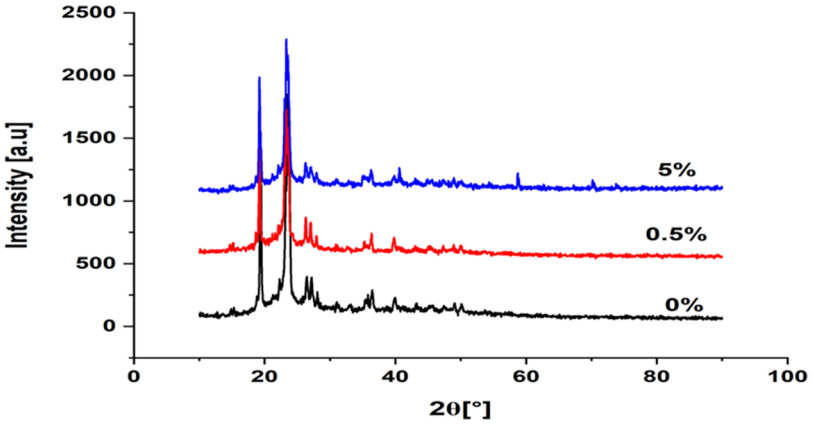

Figure 14. XRD pattern of SPE with different wt % of MnO_2.

to be more than Avogadro's number, which has no physical significance.

When we applied the formula of Rice and Roth, the *n* variation is shown in Figure 10. The increase in *n* is relatively

https://doi.org/10.1021/acsomega.3c05006
ACS Omega 2023, 8, 35256−35265

slow compared to that obtained from the S&G model, which increases in a steady manner. It may be noted that the Rice and Roth model is actually meant for crystalline superionic conductors, which are different from the actual composition of the polymer matrix. However, the concept of a mean free path, or "free ion," within the polymer matrix is feasible. The ion can and does hop from one oxygen site to another, which is analogous to the hopping from one equi-energy site to another in a crystal. Also, the matrix is not fully amorphous at temperatures before melting. Thus, the R&R model can be extended to the polymer electrolytes that are partially crystalline, irrespective of their conductivity value. Therefore, the transport theory in terms of eq 4 can be extended to the partially crystalline polymer−salt matrix.

3.1.3.2.(b) Mobility

Our material is amorphous in nature, while the Rice and Roth model is fundamentally designed for crystalline materials, so this model has some limitations for our system. In the crystalline regions of PEO and PEO−salt complexes, ions do conduct, but their conductivity is very low.[8,19] Prior to melting, the matrix was crystalline, resulting in low conductivity and constant mobility. However, after melting, the entire matrix becomes amorphous, and the velocity of ions cannot increase further. Consequently, mobility becomes almost constant. Applying the Trukhan model shows that mobility remains almost unchanged with temperature. The space charge around the MnO_2 filler for ions, the percolation path, and its width remain fixed. The width determines how many ions can migrate through at any given instant, leading to a fixed number of ions for percolation and hence constant mobility.

As the Schutt and Gerdes model is mainly based on the glassy matrix, when we apply the formula, we can see in Figures 10 and 11 that mobility starts to decrease, and a small peak at around 60° corresponds to the melting of the crystalline part of the polymer−salt complex, and a wide peak at around 70° corresponds to the melting of the crystalline PEO network, as shown in Figure 11. Mobility decreases at high temperatures because of the formation of ion pairs, and ions start forming bunches together; hence, mobility starts to decrease because cluster formation occurs.[31]

3.1.4. Dielectric Constant. Figure 12a,b displays the dielectric constant as a function of frequency for various wt % of MnO_2. Here, ε' and ε'' are the real and imaginary parts of the dielectric constant, respectively. It was observed that ε' and ε'' values decrease with increasing frequency and saturate at high frequencies. Also, in Figure 12a, the inset shows the graph between log ε' and frequency. Through the inset graph, it can be seen that at a lower frequency, the value decreases very fast and becomes saturated, approaching a higher frequency. There is no additional ion diffusion in the direction of the electric field because the ions are unable to react to the applied field due to the quick direction change. Additionally, because there was not enough time for the ions to properly build up at the electrodes, the dielectric permittivity decreased.[32] The production of free charges at the electrolyte−electrode interface causes ε'' to have a high value at low frequencies, as shown in Figure 12b. However, in the high-frequency range, the value of ε'' decreases because there are fewer charge carriers at the electrode and electrolyte contact.[33]

3.1.5. Modulus Study. Figure 13a,b shows the real and imaginary modulus components, respectively. We saw that the maximum's position has moved to the higher frequency side, which suggests the presence of a relaxation event and supports the system's ion-conducting nature. The relaxation is reduced as a result of the peak shifting from the lower frequency side to the higher frequency side with increased MnO_2 concentration, which indicates quicker ionic mobility. Due to the polarization effect or charge accumulation at the electrode−electrolyte interface, the M′ and M″ values at lower frequencies become zero.[33]

3.2. Structural Studies. *3.2.1. XRD Study.* The XRD patterns of PEO, NaI, and MnO_2 are observed at 0, 0.5, and 5 wt % MnO_2, as shown in Figure 14. Pure PEO has two high-intensity diffraction peaks in its X-ray diffraction pattern at 19.6 and 23.72°,[34] which are observed in all of our samples. In PEO peaks, we observed a halo. The halo indicates the amorphicity involved in the polymer matrix. The largest halo is observed in 0.5% MnO_2, which fits with our previous comments about the amorphicity of the samples and their conductivity. The smallest halo observed in the sample with 5% MnO_2[24] has shown low conductivity, as discussed above.

4. CONCLUSIONS

The concentration of MnO_2 directly affects the conductivity, with the highest conductivity occurring at 0.5 wt %. The conductivity also increases as the temperature increases. Models such as the Trukhan, Schutt and Gerdes, and Rice and Roth models help establish a correlation between mobility, charge carriers, and conductivity at both room temperature and increasing temperatures. The conductivity is dependent on the charge carriers and mobility, and the Trukhan model is best suited for partially crystalline polymer composite matrices. However, the S&G model, which assumes a completely amorphous matrix, may result in a value of n that exceeds Avogadro's number. The Rice and Roth model is only valid for completely crystalline matrixes and not partially crystalline polymer electrolytes.

■ ASSOCIATED CONTENT

Supporting Information

The Supporting Information is available free of charge at https://pubs.acs.org/doi/10.1021/acsomega.3c05006.

Detailed information about DTA and FTIR studies, along with graphs (PDF)

■ AUTHOR INFORMATION

Corresponding Author

Bhaskar Bhattacharya − *Department of Physics, MMV, Banaras Hindu University, Varanasi 221005, India*; Email: bhaskar.phys@bhu.ac.in, bhaskarmiet@gmail.com

Authors

Meenakshi − *Department of Physics, MMV, Banaras Hindu University, Varanasi 221005, India*

Amit Saxena − *Department of Physics, IPS Academy, Jhabua 457661, India*; orcid.org/0000-0003-2590-7234

Complete contact information is available at: https://pubs.acs.org/10.1021/acsomega.3c05006

Notes

The authors declare no competing financial interest.

https://doi.org/10.1021/acsomega.3c05006
ACS Omega 2023, 8, 35256−35265

■ ACKNOWLEDGMENTS

The authors express their gratitude for the financial support provided as an incentive grant to senior faculty members (6532) by the Institute of Eminence at BHU.

■ REFERENCES

(1) Yang, X.; Liu, J.; Pei, N.; Chen, Z.; Li, R.; Fu, L.; Zhang, P.; Zhao, J. *The Critical Role of Fillers in Composite Polymer Electrolytes for Lithium Battery*; Springer Nature Singapore, 2023; Vol. *15*.
(2) Ma, Y.; Bi, R.; Yang, M.; Wei, P.; Qi, J.; Wang, J.; Yu, R.; Wang, D. Hollow Multishelled Structural ZnO Fillers Enhance the Ionic Conductivity of Polymer Electrolyte for Lithium Batteries. *J. Nanopart. Res.* **2023**, *25*, No. 14.
(3) Liu, S.; Liu, W.; Ba, D.; Zhao, Y.; Ye, Y.; Li, Y.; Liu, J. Filler-Integrated Composite Polymer Electrolyte for Solid-State Lithium Batteries. *Adv. Mater.* **2023**, *35*, No. e2110423.
(4) Sekhon, S. S.; Sandhar, G. S. Effect of SiO2 on Conductivity of PEO AgSCN Polymer Electrolytes. *Eur. Polym. J.* **1998**, *34*, 435−438.
(5) Bhattacharya, B.; Tomar, S. K.; Pandey, S. P.; Rhee, H. W.; Singh, P. K. Porous Nanocrystalline TiO2 Electrode and Poly(N-Methyl 4-Vinylpyridine Iodide): Ionic Liquid Solid Polymer Electrolyte for Device Application. *Int. J. Nanotechnol.* **2012**, *9*, 1030−1039.
(6) Pandey, G. P.; Hashmi, S. A.; Agrawal, R. C. Hot-Press Synthesized Polyethylene Oxide Based Proton Conducting Nanocomposite Polymer Electrolyte Dispersed with SiO2 Nanoparticles. *Solid State Ionics* **2008**, *179*, 543−549.
(7) Liang, C. C.; Joshi, A. V.; Hamilton, N. E. Solid-State Storage Batteries. *J. Appl. Electrochem.* **1978**, *8*, 445−454.
(8) Saxena, A.; Bhattacharya, B. Studies on CuI Dispersed Mixed (Ion + Electron) Conducting Composite Polymer Electrolyte System. *J. Electron. Mater.* **2018**, *47*, 6163−6170.
(9) Singh, R.; Singh, P. K.; Singh, V.; Bhattacharya, B. Quantitative Analysis of Ion Transport Mechanism in Biopolymer Electrolyte. *Opt. Laser Technol.* **2019**, *113*, 303−309.
(10) Saxena, A.; Malhotra, K.; Jaithliya, M.; Agarwal, S.; Bhattacharya, B. Analytical Analysis of Concentration of Charge Carriers in Polymer Electrolytes through Different Models. *Mater. Today: Proc.* **2022**, *68*, 2726−2729.
(11) Hama, P. O.; Brza, M. A.; Tahir, H. B.; Aziz, S. B.; Al-Asbahi, B. A.; Ahmed, A. A. A. Simulated EIS and Trukhan Model to Study the Ion Transport Parameters Associated with Li+ Ion Dynamics in CS Based Polymer Blends Inserted with Lithium Nitrate Salt. *Results Phys.* **2023**, *46*, No. 106262.
(12) Wang, Y.; Agapov, A. L.; Fan, F.; Hong, K.; Yu, X.; Mays, J.; Sokolov, A. P. Decoupling of Ionic Transport from Segmental Relaxation in Polymer Electrolytes. *Phys. Rev. Lett.* **2012**, *108*, No. 088303.
(13) Gupta, S.; Singh, P. K.; Bhattacharya, B. Change in Charge Carrier Dynamics by Incorporating Ionic Liquid into Poly Ethylene Oxide−Based Sodium Acetate Polymer Electrolytes. *High Perform. Polym.* **2022**, *34*, 683−690.
(14) Munar, A.; Andrio, A.; Iserte, R.; Compañ, V. Ionic Conductivity and Diffusion Coefficients of Lithium Salt Polymer Electrolytes Measured with Dielectric Spectroscopy. *J. Non-Cryst. Solids* **2011**, *357*, 3064−3069.
(15) Schütt, H.; Gerdes, E. Space-Charge Relaxation in Ionicly Conducting Oxide Glasses. I. Model and Frequency Response. *J. Non-Cryst. Solids* **1992**, *144*, 1−13.
(16) Rice, M. J.; Roth, W. L. Ionic Transport in Super Ionic Conductors: A Theoretical Model. *J. Solid State Chem.* **1972**, *4*, 294−310.
(17) Klein, R. J.; Zhang, S.; Dou, S.; Jones, B. H.; Colby, R. H.; Runt, J. Modeling Electrode Polarization in Dielectric Spectroscopy: Ion Mobility and Mobile Ion Concentration of Single-Ion Polymer Electrolytes. *J. Chem. Phys.* **2006**, *124*, No. 144903.
(18) Schütt, H.-J.; Gerdes, E. Effect of Composition on Electrical Relaxation in Potassium Borosilicate Glasses. *J. Non-cryst. Solids* **1984**, *68*, 175−191.
(19) Bruce, P. G.; Evans, J.; Vincent, C. A. Conductivity and Transference Number Measurements on Polymer Electrolytes. *Solid State Ionics* **1988**, *28*−*30*, 918−922.
(20) Ahmed, H. T.; Abdullah, O. G. Impedance and Ionic Transport Properties of Proton-Conducting Electrolytes Based on Polyethylene Oxide/Methylcellulose Blend Polymers. *J. Sci.: Adv. Mater. Devices* **2020**, *5*, 125−133.
(21) Idris, N. K.; Aziz, N. A. N.; Zambri, M. S. M.; Zakaria, N. A.; Isa, M. I. N. Ionic Conductivity Studies of Chitosan-Based Polymer Electrolytes Doped with Adipic Acid. *Ionics* **2009**, *15*, 643−646.
(22) Wimalaweera, K. K.; Seneviratne, V. A.; Dissanayake, M. A. K. L. Effect of Al_2O_3 Ceramic filler on Thermal and Transport Properties of Poly (Ethelene Oxide)-Lithium Perchlorate Solid Polymer Eletcrolyte. *Procedia Eng.* **2017**, *215*, 109−114.
(23) Dhapola, P. S.; Singh, P. K.; Bhattacharya, B.; Surana, K.; Mehra, R. M.; Gupta, M.; Singh, A.; Singh, V.; Sahoo, N. G. Electrical, Thermal, and Dielectric Studies of Ionic Liquid-Based Polymer Electrolyte for Photoelectrochemical Device. *High Perform. Polym.* **2018**, *30*, 1002−1008.
(24) Lakshmi, N.; Chandra, S. Proton Conducting Composites of Heteropolyacid Hydrates (Phosphomolybdic and Phosphotungstic Acids) Dispersed with Insulating Al2O3. *Phys. Status Solidi A* **2001**, *186*, 383−399.
(25) Lee, J. Y.; Bhattacharya, B.; Kim, D. W.; Park, J. K. Poly(Ethylene Oxide)/Poly(Dimethylsiloxane) Blend Solid Polymer Electrolyte and Its Dye-Sensitized Solar Cell Applications. *J. Phys. Chem. C* **2008**, *112*, 12576−12582.
(26) Singh, M.; Singh, V. K.; Surana, K.; Bhattacharya, B.; Singh, P. K.; Rhee, H. W. New Polymer Electrolyte for Electrochemical Application. *J. Ind. Eng. Chem.* **2013**, *19*, 819−822.
(27) Singh, R.; Pandey, S. P.; Shukla, P. K.; Tomar, S. K.; Bhattacharya, B.; Singh, P. K. Synthesis of Lead Sulphide Nanoparticles for Electrode Application of Dye Sensitized Solar Cells. *Nanosci. Nanotechnol. Lett.* **2014**, *6*, 31−36.
(28) Gupta, S.; Singh, P. K.; Bhattacharya, B. Low-Viscosity Ionic Liquid−Doped Solid Polymer Electrolytes: Electrical, Dielectric, and Ion Transport Studies. *High Perform. Polym.* **2018**, *30*, 986−992.
(29) Li, Y.; Sun, Z.; Liu, D.; Gao, Y.; Wang, Y.; Bu, H.; Li, M.; Zhang, Y.; Gao, G.; Ding, S. A Composite Solid Polymer Electrolyte Incorporating MnO2 Nanosheets with Reinforced Mechanical Properties and Electrochemical Stability for Lithium Metal Batteries. *J. Mater. Chem. A* **2020**, *8*, 2021−2032.
(30) Bhattacharya, B.; Singh, P. K.; Khan, Z. H.; Gupta, M. Comparative Photovoltaic Study of Lead and Tin Based Perovskite Sensitized Solar Cell Using Polymer Electrolyte. *Int. J. Electroact. Mater* **2017**, 13−18.
(31) Gupta, S.; Singh, P. K.; Bhattacharya, B. Charge Carriers Dynamics in PEO + NaSCN Polymer Electrolytes. *Ionics* **2018**, *24*, 163−167.
(32) Arya, A.; Sharma, A. L. Effect of Salt Concentration on Dielectric Properties of Li-Ion Conducting Blend Polymer Electrolytes. *J. Mater. Sci. Mater. Electron.* **2018**, *29*, 17903−17920.
(33) Shyly, P. M.; Karuppasamy, K.; Linda, T.; et al. Ionic Conductivity and Dielectric Studies of Chitin Nanofiber (CNF) Incorporated PMMA Based Polymer Electrolytes. *IOSR J. Appl. Phys.* **2012**, *1*, 47−51.
(34) Polu, A. R.; Rhee, H. W. The Effects of LiTDI Salt and POSS-PEG (n = 4) Hybrid Nanoparticles on Crystallinity and Ionic Conductivity of PEO Based Solid Polymer Electrolytes. *Sci. Adv. Mater.* **2016**, *8*, 931−940.

https://doi.org/10.1021/acsomega.3c05006
ACS Omega 2023, 8, 35256−35265